

R value measurements for e^+e^- annihilation at 2.60, 3.07 and 3.65 GeV

M. Ablikim¹, J. Z. Bai¹, Y. Bai¹, Y. Ban¹¹, X. Cai¹, H. F. Chen¹⁶, H. S. Chen¹, H. X. Chen¹, J. C. Chen¹, Jin Chen¹, X. D. Chen⁵, Y. B. Chen¹, Y. P. Chu¹, Y. S. Dai¹⁸, Z. Y. Deng¹, S. X. Du^{1a}, J. Fang¹, C. D. Fu¹, C. S. Gao¹, Y. N. Gao¹⁴, S. D. Gu¹, Y. T. Gu⁴, Y. N. Guo¹, Y. Q. Guo¹, Z. J. Guo^{15b}, F. A. Harris¹⁵, K. L. He¹, M. He¹², Y. K. Heng¹, H. M. Hu¹, J. H. Hu³, T. Hu¹, G. S. Huang^{1c}, X. T. Huang¹², Y. P. Huang¹, X. B. Ji¹, X. S. Jiang¹, J. B. Jiao¹², D. P. Jin¹, S. Jin¹, Y. Jin^{1d}, G. Li¹, H. B. Li¹, H. H. Li^{1e}, J. Li¹, L. Li¹, R. Y. Li¹, W. D. Li¹, W. G. Li¹, X. L. Li¹, X. N. Li¹, X. Q. Li¹⁰, Y. F. Liang¹³, B. J. Liu^{1f}, C. X. Liu¹, Fang Liu¹, Feng Liu⁶, H. M. Liu¹, J. P. Liu¹⁷, H. B. Liu^{4g}, J. Liu¹, Q. Liu¹⁵, R. G. Liu¹, S. Liu⁸, Z. A. Liu¹, F. Lu¹, G. R. Lu⁵, J. G. Lu¹, C. L. Luo⁹, F. C. Ma⁸, H. L. Ma², Q. M. Ma¹, M. Q. A. Malik¹, Z. P. Mao¹, X. H. Mo¹, J. Nie¹, S. L. Olsen¹⁵, R. G. Ping¹, N. D. Qi¹, J. F. Qiu¹, G. Rong¹, X. D. Ruan⁴, L. Y. Shan¹, L. Shang¹, C. P. Shen¹⁵, X. Y. Shen¹, H. Y. Sheng¹, H. S. Sun¹, S. S. Sun¹, Y. Z. Sun¹, Z. J. Sun¹, X. Tang¹, J. P. Tian¹⁴, G. L. Tong¹, G. S. Varner¹⁵, X. Wan¹, L. Wang¹, L. L. Wang¹, L. S. Wang¹, P. Wang¹, P. L. Wang¹, Y. F. Wang¹, Z. Wang¹, Z. Y. Wang¹, C. L. Wei¹, D. H. Wei³, Y. Weng^{1h}, N. Wu¹, X. M. Xia¹, G. F. Xu¹, X. P. Xu⁶, Y. Xu¹⁰, M. L. Yan¹⁶, H. X. Yang¹, M. Yang¹, Y. X. Yang³, M. H. Ye², Y. X. Ye¹⁶, C. X. Yu¹⁰, C. Z. Yuan¹, Y. Yuan¹, Y. Zeng⁷, B. X. Zhang¹, B. Y. Zhang¹, C. C. Zhang¹, D. H. Zhang¹, H. Q. Zhang¹, H. Y. Zhang¹, J. W. Zhang¹, J. Y. Zhang¹, X. Y. Zhang¹², Y. Y. Zhang¹³, Z. X. Zhang¹¹, Z. P. Zhang¹⁶, D. X. Zhao¹, J. W. Zhao¹, M. G. Zhao¹, P. P. Zhao¹, Z. G. Zhao¹⁶, B. Zheng¹, H. Q. Zheng¹¹, J. P. Zheng¹, Z. P. Zheng¹, B. Zhong⁹, L. Zhou¹, K. J. Zhu¹, Q. M. Zhu¹, X. W. Zhu¹, Y. S. Zhu¹, Z. A. Zhu¹, Z. L. Zhu³, B. A. Zhuang¹, B. S. Zou¹

(BES Collaboration)

¹ Institute of High Energy Physics, Beijing 100049, People's Republic of China² China Center for Advanced Science and Technology (CCAST), Beijing 100080, People's Republic of China³ Guangxi Normal University, Guilin 541004, People's Republic of China⁴ Guangxi University, Nanning 530004, People's Republic of China⁵ Henan Normal University, Xinxiang 453002, People's Republic of China⁶ Huazhong Normal University, Wuhan 430079, People's Republic of China⁷ Hunan University, Changsha 410082, People's Republic of China⁸ Liaoning University, Shenyang 110036, People's Republic of China⁹ Nanjing Normal University, Nanjing 210097, People's Republic of China¹⁰ Nankai University, Tianjin 300071, People's Republic of China¹¹ Peking University, Beijing 100871, People's Republic of China¹² Shandong University, Jinan 250100, People's Republic of China¹³ Sichuan University, Chengdu 610064, People's Republic of China¹⁴ Tsinghua University, Beijing 100084, People's Republic of China¹⁵ University of Hawaii, Honolulu, HI 96822, USA¹⁶ University of Science and Technology of China, Hefei 230026, People's Republic of China¹⁷ Wuhan University, Wuhan 430072, People's Republic of China¹⁸ Zhejiang University, Hangzhou 310028, People's Republic of China

^a Current address: Zhengzhou University, Zhengzhou 450001, People's Republic of China

^b Current address: Johns Hopkins University, Baltimore, MD 21218, USA

^c Current address: University of Oklahoma, Norman, Oklahoma 73019, USA

^d Current address: Jinan University, Jinan 250022, People's Republic of China

^e Current address: National Natural Science Foundation of China, Beijing 100085, People's Republic of China

^f Current address: University of Hong Kong, Pok Fu Lam Road, Hong Kong

^g Current address: Graduate University of Chinese Academy of Sciences, Beijing 100049, People's Republic of China

^h Current address: Cornell University, Ithaca, New York 14853, USA

Abstract

Using a data sample with a total integrated luminosity of 10.0 pb^{-1} collected at center-of-mass energies of 2.6, 3.07 and 3.65 GeV with BESII, cross sections for e^+e^- annihilation into hadronic final states (R values) are measured with statistical errors that are smaller than 1%, and systematic errors that are about 3.5%. The running strong interaction coupling constants $\alpha_s^{(3)}(s)$ and $\alpha_s^{(5)}(M_Z^2)$ are determined from the R values.

1 Introduction

The R ratio is defined as the lowest level hadronic cross section normalized by the theoretical $\mu^+\mu^-$ production cross section in e^+e^- annihilation

$$R = \frac{\sigma_{had}^0(e^+e^- \rightarrow \gamma^* \rightarrow \text{hadrons})}{\sigma_{\mu\mu}^0(e^+e^- \rightarrow \gamma^* \rightarrow \mu^+\mu^-)}, \quad (1)$$

and it is an important input parameter for precision tests of the Standard Model (SM). The errors on R value measurements below 5 GeV have a strong influence on the uncertainties of the calculated QED running electromagnetic coupling constant $\alpha(s)$, the muon anomalous magnetic moment ($g-2$) and global SM fits for the Higgs mass [1, 2, 3]. In addition, precision measurements of R values between 2.0 and 3.7 GeV provide a test of perturbative QCD and QCD sum rule calculations [4, 5, 6].

In 1998 and 1999, R value measurements were made at 91 energy points [7, 8] between 2 and 5 GeV by the BESII [9] experiment. The R values were determined from the expression

$$R_{exp} = \frac{N_{had}^{obs} - N_{bg}}{\sigma_{\mu\mu}^0 L \epsilon_{trg} \epsilon_{had}^0 (1 + \delta_{obs})}, \quad (2)$$

where N_{had}^{obs} is the number of observed hadronic events, N_{bg} is the number of QED background events surviving hadron selection (e^+e^- , $\mu^+\mu^-$, $\tau^+\tau^-$, $\gamma\gamma$, etc.), L is the integrated luminosity, ϵ_{trg} is the trigger efficiency for hadronic events, ϵ_{had}^0 is the hadronic efficiency without the

simulation of initial state radiation (ISR), and $(1 + \delta_{obs})$ is the effective ISR correction which includes the effect of radiated photons on the hadronic acceptance. The average statistical errors of the R values are 2 – 4%, and the systematical errors are 5 – 8% depending on the energy point; for the latter, the errors associated with the event selection, hadronic efficiency, and luminosity are dominant.

In 2004, large-statistics data samples were accumulated at center-of-mass energies of 2.60, 3.07 and 3.65 GeV; the total integrated luminosity was 10.0 pb^{-1} . An additional 65.2 nb^{-1} was accumulated at 2.2 GeV for the purpose of tuning the parameters of the hadronic event generator. Improvements in the event selection, tuning of generator parameters and luminosity measurement have been made in order to decrease the systematic errors. The previously used EGS-based (Electron Gamma Shower) [10] detector simulation (where hadronic interactions were parametrized but not simulated) was replaced by a GEANT3-based one [11, 12], where both electromagnetic and hadronic interactions are simulated. The consistency between data and Monte Carlo (MC) has been validated using many high purity physics channels [13]. With these improvements, the errors on the new measured R values are reduced to about 3.5%.

In this letter, improvements compared to the previous measurements are described, and the error analysis and results are reported. Finally, the strong running coupling constant $\alpha_s^{(3)}(s)$ and $\alpha_s^{(5)}(M_Z^2)$ are determined from the R values.

2 Data analysis

The analysis used for this work is similar to that used in the previous BESII R measurements [7, 8]. Two large sources of error in the measurement arise from the event selection and the determination of the hadronic efficiency; these are strongly correlated.

2.1 Selection of hadronic events

In the BEPC energy region, data collected include processes that originate from beam-beam collisions, $e^+e^- \rightarrow e^+e^-, \mu^+\mu^-, \tau^+\tau^-, \gamma\gamma, e^+e^-X$ (X means any possible final state), and hadrons (including continuum and resonant states), as well as beam associated backgrounds. The observed final state charged particles are e, μ, π, K , and p . To test the hadron selection criteria, described below, different types of backgrounds are selected using specialized criteria, and most of them are rejected with good efficiency [7, 8, 14].

The candidate hadronic events are classified by their number of charged tracks. The selection of hadronic events is done in two successive steps: one at the track level and the other at the event level.

(I) Track level: only charged tracks that are well fitted to a helix are considered; the point of closest approach of the track, signified by (V_x, V_y, V_z) , must be within 2 cm of the beam-line in the x - y plane with no restriction on V_z ; the angle between the track and the z axis is limited by the coverage of the main drift chamber (MDC) to be within $|\cos \theta| < 0.84$; a momentum cut $p < E_b(1 + 0.1\sqrt{1 + E_b^2})$ removes tracks with unphysically high momentum (E_b is the beam energy in units of GeV); a time of flight (TOF) requirement $t_{TOF} \leq t_p + 2 \text{ ns}$ is applied

to reject events with unphysical times (t_p is the expected value for a proton with momentum p); the energy deposited in the barrel shower counter (BSC), E_{BSC} , must be less than the minimum of 1 GeV and $0.6E_B$; and the number of hit layers in the muon counter must be smaller than 3.

A neutral cluster in the BSC is considered to be a photon candidate if the angle between the nearest charged track and the cluster is greater than 25° ; the difference between the angle of the cluster development direction and the photon emission direction in the BSC is less than 30° ; and the number of hit layers in the BSC is larger than two.

(II) Event level: the requirement that the total deposited energy, E_{BSC}^{sum} , is greater than the maximum of 0.5 GeV and $0.28E_b$ eliminates most of the beam-associated backgrounds. The selected tracks must not all point into the forward ($\cos\theta > 0$) or the backward ($\cos\theta < 0$) hemisphere. For multi-track events ($n_{ch} \geq 3$), no further requirement is used. For two-track events, the two charged tracks cannot be back-to-back, so the angle between them is required to be less than 165° , and there must be at least two isolated photons with energy $E_\gamma > 0.1$ GeV that are well separated from charged tracks, *i.e.* the distance between the neutral and charged tracks at the first layer of the BSC must be larger than 34 cm in the x - y plane, or larger than 60 cm in the z direction.

The above described selection criteria for hadronic events with $n_{ch} \geq 2$ are almost the same as used in the previous measurements [7, 8]. In the BEPC energy region, the number of events with one observed/reconstructed charged track in BESII accounts for about 8-13% of all hadronic events. The omission of one-track (and zero-track) hadronic events introduces some uncertainty in the tuning the parameters of the hadronic event generator parameters; this in turn induces a sizable systematic error in the hadronic efficiency. However, for single-track events, contamination from beam-associated backgrounds is significant. Therefore, a more restrictive hadronic event selection is applied [14]: the event must have one charged track that is well fitted to a helix (the event can have additional any number of charged tracks with poor helix fits). If this charged track is identified as e^\pm , the event is rejected. If its momentum is in the range $p > 1$ GeV and the number of hit layers in the muon counter is larger than 1, the event is also rejected. For each single-track event, the number of photons with energy $E_\gamma > 0.1$ GeV should be two or more. To further suppress background from fake photons, only events with one well fitted charged track and at least one reconstructed π^0 are considered as single-track hadronic events. A 1-C fit is applied under the $\pi^0 \rightarrow \gamma\gamma$ hypothesis. For candidates with more photons ($n_\gamma \geq 3$), the $\gamma\gamma$ pair combination with the smallest χ^2 is chosen. The χ^2 probability for the 1-C fit is required to be larger than 1%. Figure 2(h) shows the invariant $\gamma\gamma$ mass distribution for one-track events satisfying requirements for data and MC (the MC is normalized to the integrated luminosity of the data). The good agreement indicates that the rate of one-track events in data and MC are commensurate, and the residual beam-associated background is small.

For selected events, the weighted average vertex position, \bar{V}_z , is determined using

$$\bar{V}_z = \frac{\sum_{i=1}^n V_z(i)/\tilde{\chi}_i^2}{\sum_{i=1}^n 1/\tilde{\chi}_i^2}, \quad (3)$$

where $V_z(i)$ is the z coordinate of the i th selected track, χ_i^2 is the track fitting chi-square,

$\tilde{\chi}_i^2 = \chi_i^2/n_{D.O.F.}$, $n_{D.O.F.}$ is the number of degrees of freedom, and n is the number of tracks in the event. Figure 1 shows the \overline{V}_z distributions for candidate hadronic events (including the residual beam-associated and QED backgrounds) at 2.6, 3.07 and 3.65 GeV. Signal events produced by e^+e^- collisions originate near the collision point (in the neighborhood of $z = 0$), and the non-beam-beam backgrounds, such as those from beam-gas and beam-wall scattering, are distributed all along the beam direction (In order to show the shape of the \overline{V}_z distribution of residual beam-associated backgrounds clearly, a logarithmic vertical scale is used). The number of observed hadronic events N_{had}^{obs} is determined by fitting the \overline{V}_z distribution with a Gaussian to describe the hadronic events and an m -th degree polynomial for the residual beam associated backgrounds.

The numbers of residual QED background events, N_{bg} in Eq.(2), are determined from MC simulations using QED event generators with an accuracy of 1% [15], where

$$N_{bg} = L[\epsilon_{ee}\sigma_{ee} + \epsilon_{\mu\mu}\sigma_{\mu\mu} + \epsilon_{\tau\tau}\sigma_{\tau\tau} + \epsilon_{\gamma\gamma}\sigma_{\gamma\gamma}]. \quad (4)$$

Here σ_{ee} is the production cross section for Bhabha events given by the corresponding generator, ϵ_{ee} is the efficiency for Bhabha events that pass the hadronic event selection criteria, and other symbols have corresponding meanings. The values of ϵ_{ee} and $\epsilon_{\mu\mu}$ are about 5×10^{-4} , and $\epsilon_{\tau\tau}$ is 36.45% at 3.65 GeV. The errors on N_{bg} are given in Table 2. The amount of background from $e^+e^- \rightarrow e^+e^-X$ that survives hadron selection is much smaller than 1% of N_{bg} and is neglected.

2.2 Tuning the LUARLW parameters

The hadronic efficiency is determined using the LUARLW hadronic event generator [16]. The physical basis of LUARLW is the Lund area law [17]. The production of hadrons is described as the fragmentation of a semi-classical relativistic string [18], and the quark components of the string and decays of unstable particles are handled by subroutines in JESTSET [19, 20, 21].

Both generators LUARLW and JETSET have some phenomenological parameters that have to be determined from data. The important parameters in JETSET are $PARJ(1 - 3)$, which are responsible for the suppression of diquark-diantiquark pair production, quark pair production, and the extra suppression of strange diquark production respectively, and $PARJ(11 - 17)$, which control the relative probabilities of different spin mesons. The values of these parameters have been tuned with LEP data, as well as with information from lower energy e^+e^- colliders [22]. The generator LUARLW has also been tuned with BES data taken at 2.2, 2.6, 3.07 and 3.65 GeV. The tuned parameters for the Lund area law are mainly the dynamical parameter b and those related to the initial multiplicity distributions (including neutral clusters and charged tracks) from the string decay [16].

The basic method is to find a set of parameters that make various distributions (especially those related to the hadronic selection) simulated by MC agree well with experimental data at all of the measured energy points. The distributions used for the data–MC comparison are: the multiplicities of charged tracks and neutral clusters, the V_{x-y} and V_z coordinates of charged tracks, the charged track momentum, the polar-angle θ between tracks and the beam

direction, the deposited energy in the BSC, the time of flight, and fractions of π^\pm , K^\pm , and some other short-lived particles (π^0 , K_S , ϕ , Λ), etc.. With these distributions, the systematic errors corresponding to each criteria used in the hadronic event selection can be determined. Figure 2 shows, for example, some comparisons between data and the LUARLW MC at 3.65 GeV, where reasonable agreement is evident. More distributions at other energy points are also compared, which can be found in Refs. [14, 23].

The parameters for detector simulation are studied using data. The constant files for dead and hot channels, and the detailed detector responses are inputs for detector simulations.

2.3 Trigger, luminosity and ISR

The trigger conditions are almost the same as those used for the R measurements reported in Refs. [7, 8], and the details about the values and errors of the trigger efficiency are described in Refs. [24]. Since one-track hadronic events are also included in this measurement, the TOF back-to-back hit trigger requirement is not used, thereby making the trigger conditions somewhat looser than before. The trigger table used in data taking is given in Ref. [14]. The trigger efficiencies ϵ_{trg} for hadronic events is determined as 99.8%, and its associated errors is conservatively estimated to be 0.5%.

The integrated luminosity L is measured with wide-angle ($|\cos\theta| < 0.6$) Bhabha events. The measurement method is similar to that described in Refs.[7, 8]. The Bhabha events are selected using only BSC information, and the simulation of the BSC is significantly improved by the package (SIMBES) described in [13], which provides better consistency between MC and data. In addition, the BSC selection efficiencies, determined by simulation, are corrected using correction factors determined with another Bhabha sample, that is selected using only MDC information. The efficiency correction factors range from 0.994 to 1.026 with an uncertainty of about 1.4% for the different energy points. In addition, the contribution from $e^+e^- \rightarrow \gamma\gamma$ is subtracted explicitly. As a result, the precision of the luminosity determined is significantly improved, and the systematic uncertainties are about 2%. For example, at 2.6 GeV the systematic error is 1.9%, of which the trigger efficiency contributes 0.5%, the MC generator 0.5%, event selection 1.2%, and the Bhabha correction 1.3%.

An $\mathcal{O}(\alpha^3)$ Feynman-diagram-based calculation for the initial state radiative (ISR) correction is used in both the calculation of the ISR factor ($1 + \delta_{obs}$) and the simulation of radiative events by LUARLW. A detailed description of the ISR treatment can be found in Refs. [25, 26, 27, 28, 29]. In the ISR simulations and calculations, the contributions from both continuum and resonances are considered. The inclusive hadronic cross section below 5 GeV uses the experimental value, and above 5 GeV uses the theoretical value predicted by QCD [30]. The quantities related to the narrow J/ψ and ψ' are treated analytically.

Figure 3 shows the detection efficiencies for hadronic events simulated with LUARLW for the cases where an initial-state e^+ or e^- radiates a photon with energy fraction $k \equiv E_\gamma/E_b$ and those events with $n_{ch} \geq 1$ are selected. Curves fitted to $\epsilon(k)$ are used in the calculation of $(1 + \delta_{obs})$ at different energies. The values of $(1 + \delta_{obs})$ and their errors are listed in Tables 1 and 2, respectively.

3 Error analysis

The Feynman-diagram-based ISR simulated angle and momentum distributions for the radiated photon are built into LUARLW, which allows the hadronic efficiency $\bar{\epsilon}_{had}$ including radiative effects to be obtained, averaging over the ISR spectrum. The number of hadronic events N_{had}^{obs} , the hadronic efficiency $\bar{\epsilon}_{had}$, and their errors are correlated. The equivalent number of hadronic events, which corresponds to the number of hadronic events produced at the collision point, is defined as

$$N_{had} = \frac{N_{had}^{obs}}{\bar{\epsilon}_{had}}. \quad (5)$$

The combined systematic error associated with the event selection and hadronic efficiency is denoted as ΔN_{had} . This error is caused by discrepancies between data and MC samples for the hadronic selection criteria discussed in Section 2.1. In addition, an uncertainty associated with the parameters of the MC hadronization model is estimated to be about 1% by comparing different sets of tuned parameters, and is included in the error of the hadronic event efficiency.

The error on N_{had}^{obs} due to the choice of the degree of the polynomial used in the fitting is less than 0.7%. The fit errors for N_{had}^{obs} , which are calculated from the uncertainties in the fitted parameters of the Gaussian signal peaks, are 1.34% at 2.6 GeV, 1.11% at 3.07 GeV, and 0.73% at 3.65 GeV. The total ΔN_{had} is the quadratic sum of all fractional errors.

The uncertainty in the effective ISR factor $(1 + \delta_{obs})$ due to errors of the hadronic cross sections at the different effective energies for radiative events is considered (the errors on the hadronic cross section given in the PDG06 tables [30] are used); these decrease with increasing energy from 0.9% to 0.1%. For comparison, another approach based on structure functions [31] is also used at all energy points. The differences in the values of $(1 + \delta)$ for the two schemes are smaller than 1.1%.

A conclusion of the KLN theorem is that the radiative corrections due to final state radiation (FSR) are negligible for a measurement of the inclusive hadronic cross section that sums over all hadronic final states [32]. At the present level of precision, the FSR correction factor in Eq.(2) can be neglected. However, the absence of final state radiation in the event generator introduces some error into the determination of the hadronic event detection efficiency. The masses of the produced hadrons in the final states are much greater than that of the initial radiative e^\pm . As a result, the effect of FSR is much weaker than initial bremsstrahlung. Its influence is estimated to be 0.5% and is included in the error.

The 0-track hadronic events are not selected in this analysis, and the influence of 0-track events on the parameter tuning of LUARLW is not considered. This introduces some error into the hadronic event efficiency determination. Events with no charged tracks cannot be well separated from background. The fraction of 0-track events is estimated from the MC to be 3.4% at 2.6 GeV, 2.9% at 3.07 GeV, and 2.4% at 3.65 GeV. If the difference for 0-track events between MC and data is conservatively assumed to be 20%, the errors for the lost/unobserved 0-track events are 0.7%, 0.6% and 0.5%, respectively. The error related to 0-track events is included into the error of N_{had} defined in Eq. (5).

In this analysis, hadronic events are classified according to their number of charged tracks. Therefore, errors in the tracking efficiency σ_{trk} , the differences in the track reconstruction

efficiency between data and MC, introduce some error into the classification and counting of the number of events. For an event with n_{ch} charged tracks, the probability that n_{er} of n_{ch} tracks are wrongly constructed roughly obeys a binomial distribution $B(n_{er}; n_{ch}, \sigma_{trk})$, where the parameter $\sigma_{trk} \sim 2\%$ is the tracking efficiency error at BESII. The R value measurement is, in fact, a counting of the number of hadronic events, so only those cases where all n_{ch} tracks in an event are incorrectly reconstructed ($n_{er} = n_{ch}$) will introduce an error into ΔN_{had} . Considering the distribution of charged multiplicity $P(n_{ch})$ for the inclusive hadronic sample (such as shown in Figure 2(a)), the effective error of tracking efficiency is

$$\Delta\epsilon_{trk} = \sum_{n_{ch} \geq 1} P(n_{ch}) B(n_{er} = n_{ch}; n_{ch}, \sigma_{trk}). \quad (6)$$

The estimated values of $\Delta\epsilon_{trk}$ are listed in Table 2. Since the fraction of single-track events decreases with increasing center-of-mass energy, the error $\Delta\epsilon_{trk}$ also decreases with energy.

The errors on the R values are determined with Eq. (2) (including all errors analyzed in last section and estimated by Eq. (6)). The final R values are $2.18 \pm 0.02 \pm 0.08$ at 2.6 GeV, $2.13 \pm 0.02 \pm 0.07$ at 3.07 GeV, and $2.14 \pm 0.01 \pm 0.07$ at 3.65 GeV, which are summarized in Table 1.

As a cross check, the R values are determined using the relation

$$R_{exp} = \frac{N_{had}^{obs} - N_{bg}}{\sigma_{\mu\mu}^0 L \epsilon_{trg} \bar{\epsilon}_{had} (1 + \delta)}, \quad (7)$$

where $\bar{\epsilon}_{had}$ is the hadronic efficiency averaged over all of the ISR spectrum, and $(1 + \delta)$ is the corresponding theoretical ISR factor. The ISR scheme used to simulate $\bar{\epsilon}_{had}$, ϵ_{had}^0 and to calculate $(1 + \delta)$ and $(1 + \delta_{obs})$ are the same in order to keep the consistency between theoretical calculation and simulation. The R values determined with Eq. (7) are $2.17 \pm 0.01 \pm 0.07$ at 2.6 GeV, $2.13 \pm 0.01 \pm 0.07$ at 3.07 GeV, and $2.16 \pm 0.01 \pm 0.08$ at 3.65 GeV. The mean R values obtained using Eqs. (2) and (7) are consistent to within 1%.

A cross check is also made by selecting hadronic events with $n_{ch} \geq 2$ as was done in Refs. [7, 8]. In this case, the R values at the three energy points are $2.20 \pm 0.02 \pm 0.08$, $2.13 \pm 0.02 \pm 0.07$, and $2.15 \pm 0.01 \pm 0.08$, respectively. The differences in the mean R values determined by selecting hadronic events with $n_{ch} \geq 1$ and $n_{ch} \geq 2$ are consistent within 1%.

4 Results and discussion

Tables 1 and 2 list the quantities used in the determination of R using Eq. (2) and the contributions to the total error. The results are shown in Fig. 4, together with previous measurements. The errors on the R values reported here are about 3.5%. The R values are consistent within errors with the prediction of perturbative QCD [4].

Compared with our previous results [7, 8], the measurement precision has been improved due to three main refinements to the analysis: (1) the simulation of BES including both of the hadronic and electromagnetic interactions with a GEANT3 based package SIMBES that has a more detailed geometrical description and matter definition for the sub-detectors; (2) large

data samples are taken at each energy point, with statistical errors smaller than 1%; (3) the selected hadronic event sample is expanded to include one-track events, which supplies more information to the tuning of LUARLW, and results in the improved values of parameters and hadronic efficiency.

In another BESII work, parts of the data sample taken at 3.65 GeV with a luminosity of 5.536 pb^{-1} and at 3.665 GeV with a luminosity of 998.2 nb^{-1} are used, the hadronic events with more than 2-tracks ($n_{ch} \geq 3$) are selected, and the averaged R value is $R = 2.218 \pm 0.019 \pm 0.089$ which has an error of 4.1% [33].

Based on the R values in this work and the perturbative QCD expansion that computes $R_{QCD}(\alpha_s)$ to $\mathcal{O}(\alpha_s^3)$ [34], the strong running coupling constant $\alpha_s^{(3)}(s)$ can be determined at each energy point [35, 36]. The obtained $\alpha_s^{(3)}(s)$ values are evolved to 5 GeV, and the weighted average of the measurements $\bar{\alpha}_s^{(4)}(25 \text{ GeV}^2)$ is listed in Table 3. When evaluated at the M_Z scale, the resulting value is $\alpha_s^{(5)}(M_Z^2) = 0.117^{+0.012}_{-0.017}$, which agrees with the world average value within the quoted errors [4].

Table 1: Items used in the determination of R at each energy point.

$E_{cm}(\text{GeV})$	$L(\text{pb}^{-1})$	N_{had}^{obs}	N_{bg}	$\epsilon_{had}^0(\%)$	$(1 + \delta_{obs})$	R	σ_{sta}	σ_{sys}
2.60	1.222	24026	193	63.81	1.08	2.18	0.02	0.08
3.07	2.291	33933	208	67.63	1.11	2.13	0.02	0.07
3.65	6.485	83767	4937	71.83	1.21	2.14	0.01	0.07

Table 2: Summary of the systematic errors (%).

$E_{cm}(\text{GeV})$	L	N_{had}	N_{bg}	$\Delta\epsilon_{trk}$	ϵ_{trg}	$(1 + \delta_{obs})$	Total
2.60	2.00	2.79	0.05	0.32	0.50	1.18	3.68
3.07	1.96	2.53	0.05	0.29	0.50	1.15	3.45
3.65	1.38	2.74	0.35	0.26	0.50	1.10	3.33

Table 3: $\alpha_s(s)$ determined from R values at 2.600, 3.070, and 3.650 GeV, and evolved to 5 GeV. The first and second errors are statistical and systematic, respectively. Shown in the last two columns are the weighted averages of the three measurements at 5 GeV and M_Z .

$\sqrt{s}(\text{GeV})$	$\alpha_s^{(3)}(s)$	$\alpha_s^{(4)}(25\text{GeV}^2)$	$\bar{\alpha}_s^{(4)}(25\text{GeV}^2)$	$\alpha_s^{(5)}(M_Z^2)$
2.60	$0.266^{+0.030+0.125}_{-0.030-0.116}$	$0.212^{+0.018+0.068}_{-0.019-0.086}$	$0.209^{+0.044}_{-0.050}$	$0.117^{+0.012}_{-0.017}$
3.07	$0.192^{+0.029+0.103}_{-0.029-0.101}$	$0.169^{+0.022+0.074}_{-0.023-0.086}$		
3.65	$0.207^{+0.015+0.104}_{-0.015-0.104}$	$0.189^{+0.012+0.082}_{-0.013-0.091}$		

The BES collaboration thanks the staff of BEPC and computing center for their hard efforts. BES collaboration also thanks B. Andersson for helping in the development of generator LUARLW during 1998-1999. This work is supported in part by the National Natural Science Foundation of China under contracts Nos. 19991480, 19805009, 19825116, 10491300, 10225524, 10225525, 10425523, 10625524, 10521003, the Chinese Academy of Sciences under contract No. KJ 95T-03, the 100 Talents Program of CAS under Contract Nos. U-11, U-24, U-25, and the Knowledge Innovation Project of CAS under Contract Nos. U-602, U-34 (IHEP), the National Natural Science Foundation of China under Contract No. 10225522 (Tsinghua University), and the Department of Energy under Contract No. DE-FG02-04ER41291 (U. Hawaii).

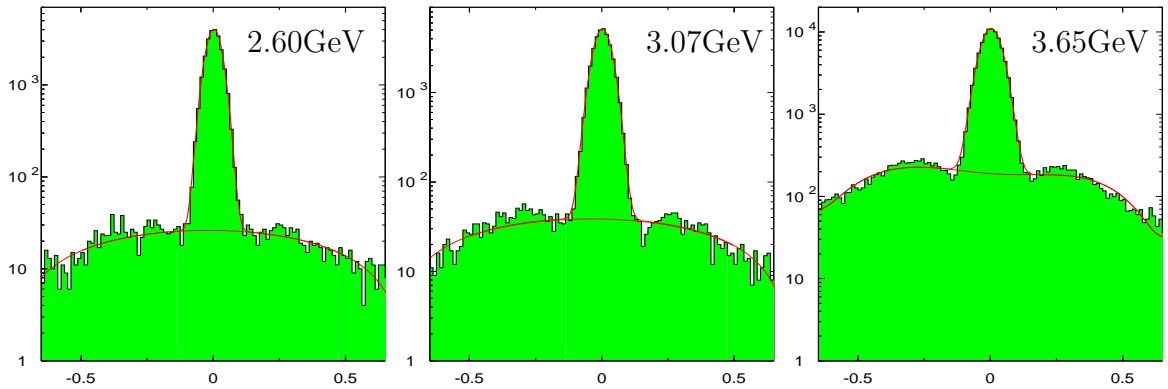


Figure 1: Distributions of \overline{V}_z for candidate hadronic events. The distributions are fitted by a Gaussian to represent the signal and a polynomial to describe the residual beam-associated backgrounds.

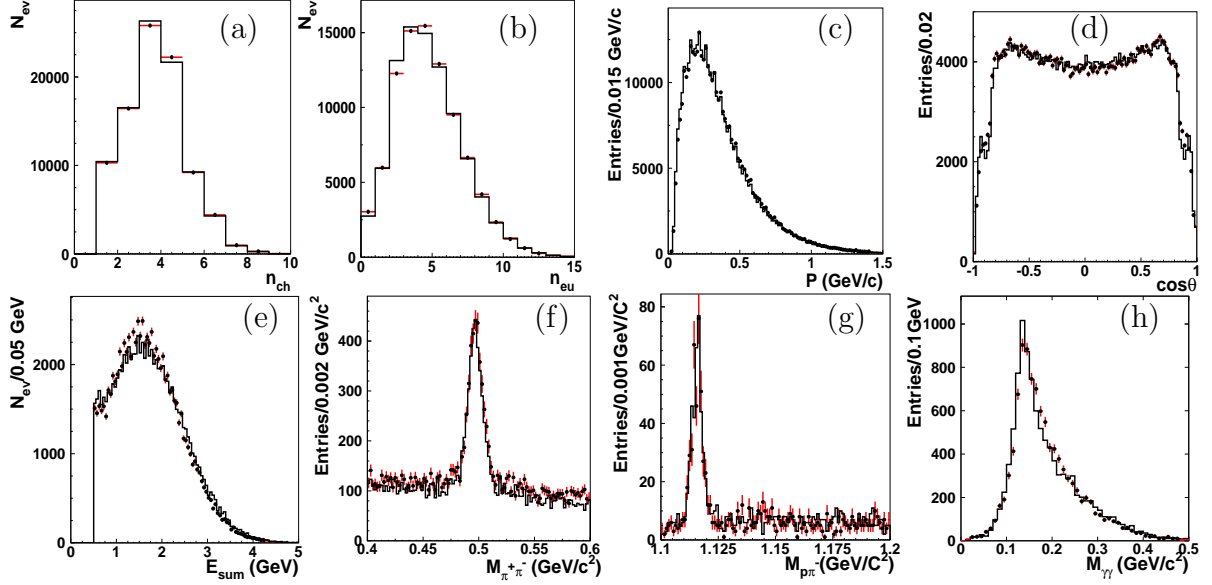


Figure 2: The normalized distributions for data (dots with error bars) and the LUARLW MC (histograms) at 3.65 GeV with full detector simulation: (a) multiplicity of charged tracks; (b) multiplicity of neutral clusters; (c) momenta p of charged tracks; (d) polar-angles between charged tracks and beam direction, $\cos\theta$; (e) deposited energies in the BSC; invariant masses of (f) $K_S \rightarrow \pi^+\pi^-$; (g) $\Lambda \rightarrow p\pi^-$ and (h) $\pi^0 \rightarrow \gamma\gamma$ decays respectively.

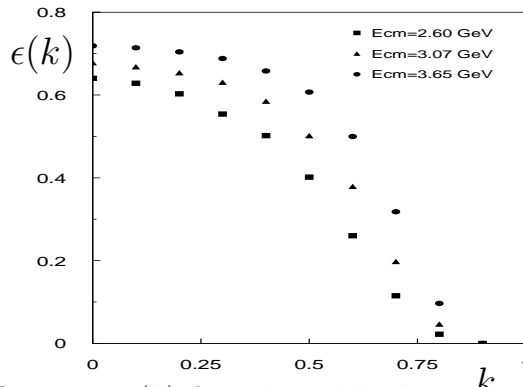


Figure 3: Radiative efficiencies $\epsilon(k)$ for selected hadronic k events with $n_{ch} \geq 1$ at some values of k .

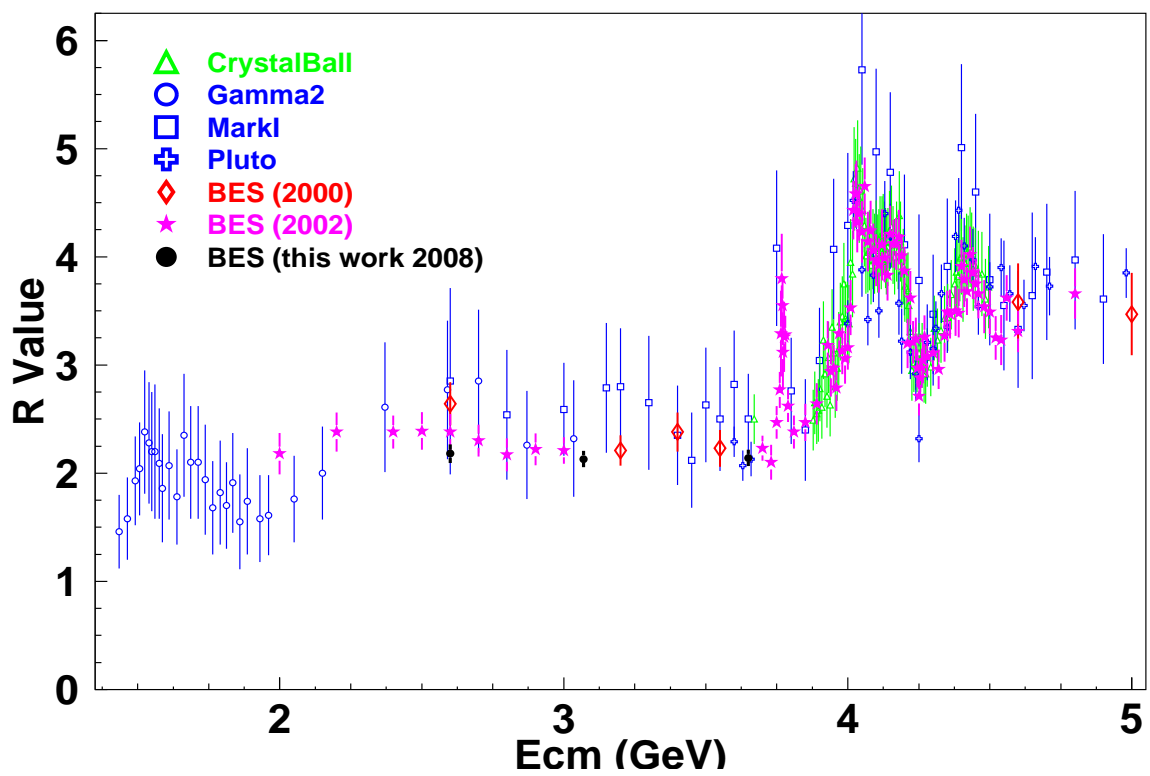


Figure 4: R values reported here together with previous measurements below 5 GeV.

References

- [1] B. Pietrzyk, Nucl. Phys. B (Proc. Suppl.) **162**, 18 (2006).
- [2] F. Jegerlehner, Nucl. Phys. B (Proc. Suppl.) **162**, 22 (2006).
- [3] F. Ambrosino *et al.*, hep-ex/0603056, and references therein.
- [4] C. Amsler *et al.*, Phys. Lett. B **667**, 122 (2008).
- [5] M. Davier *et al.*, Phys. Lett. **B 419**, 419 (1998).
- [6] M. Davier *et al.*, Eur. Phys. J. **C 27**, 497 (2003).
- [7] J.Z. Bai *et al.*, BES Collaboration, Phys. Rev. Lett. **84**, 594 (2000).
- [8] J.Z. Bai *et al.*, BES Collaboration, Phys. Rev. Lett. **88**, 101802 (2002).
- [9] J. Z. Bai *et al.*, BES Collaboration, Nucl. Instr. Meth. A **458**, 627 (2001).
- [10] W. R. Nelson *et al.*, The EGS4 Code System, SLAC-265, 1992.
- [11] CERN Program Library Long Writeup W5013, CERN, Geneva, Switzerland, 1993.
- [12] <http://wwwasdoc.web.cern.ch/wwwasdoc/>.
- [13] M. Ablikim *et al.*, BES Collaboration, Nucl. Instrum. Meth. A **552**, 344 (2005).
- [14] H. Hu *et al.* High Energy Physics and Nuclear Physics **31**, 802 (2007).
- [15] These generators are based on the calculation by the references: F. A. Berends *et al.*, Nucl. Phys. **B57**, 381 (1973); Nucl. Phys. **B68**, 451 (1974); Nucl. Phys. **B177**, 237 (1981); Nucl. Phys. **B228**, 537 (1983).
- [16] H.M. Hu *et al.*, High Energy Phys. and Nucl. Phys. **25**, 1035 (2001) (in Chinese).
- [17] B. Andersson and H. Hu, hep-ph/9810285.
- [18] B. Andersson, The Lund Model, Cambridge University Press (1998).
- [19] T. Sjöstrand, CERN-TH.7112/93.
- [20] T. Sjöstrand, Computer Physics Commun. **39**, 347 (1986).
- [21] T. Sjöstrand, Computer Physics Commun. **43**, 367 (1987).
- [22] Armin Böhrer, Phys. Rep. **191**, 107 (1997).
- [23] Y. Weng *et al.*, High Energy Physics and Nuclear Physics **31**, 703 (2007).
- [24] G.S.Huang *et al.*, High Energy Physics and Nuclear Physics **25**, 889 (2001)

- [25] A. Osterheld et al., SLAC-PUB-4160 (1986).
- [26] C. Edwards et al., SLAC-PUB-5160 (1990).
- [27] H. Hu et al., High Energy Physics and Nuclear Physics **25**, 701 (2001).
- [28] G. Bonneau and F. Martin, Nucl. Phys. **B27**, 381 (1971).
- [29] F. A. Berends and R. Kleiss, Nucl. Phys. **B178**, 141 (1981).
- [30] Particle Data Group, Jour. Phys. **33**, (2006)116
- [31] E. A. Kureav and V. S. Fadin, Sov. Nucl. Phys. **41**, 466 (1985).
- [32] Y. S. Tsai, SLAC-PUB-3129, May 1983.
- [33] M. Ablikim *et al.*, BES Collaboration, Phys. Lett. **B641**, 145 (2006).
- [34] S. G. Gorishnii, *et al.*, Phys. Let. **B259**, 144 (1991).
- [35] J. H. Kühn and M. Steinhauser, arXiv:hep-ph/0109084 v3 (2002).
- [36] J. Hu et al., High Energy Physics and Nuclear Physics **31**, 1 (2007).

R value measurements for e^+e^- annihilation at 2.60, 3.07 and 3.65 GeV

M. Ablikim¹, J. Z. Bai¹, Y. Bai¹, Y. Ban¹¹, X. Cai¹, H. F. Chen¹⁶, H. S. Chen¹, H. X. Chen¹, J. C. Chen¹, Jin Chen¹, X. D. Chen⁵, Y. B. Chen¹, Y. P. Chu¹, Y. S. Dai¹⁸, Z. Y. Deng¹, S. X. Du^{1a}, J. Fang¹, C. D. Fu¹, C. S. Gao¹, Y. N. Gao¹⁴, S. D. Gu¹, Y. T. Gu⁴, Y. N. Guo¹, Y. Q. Guo¹, Z. J. Guo^{15b}, F. A. Harris¹⁵, K. L. He¹, M. He¹², Y. K. Heng¹, H. M. Hu¹, J. H. Hu³, T. Hu¹, G. S. Huang^{1c}, X. T. Huang¹², Y. P. Huang¹, X. B. Ji¹, X. S. Jiang¹, J. B. Jiao¹², D. P. Jin¹, S. Jin¹, Y. Jin^{1d}, G. Li¹, H. B. Li¹, H. H. Li^{1e}, J. Li¹, L. Li¹, R. Y. Li¹, W. D. Li¹, W. G. Li¹, X. L. Li¹, X. N. Li¹, X. Q. Li¹⁰, Y. F. Liang¹³, B. J. Liu^{1f}, C. X. Liu¹, Fang Liu¹, Feng Liu⁶, H. M. Liu¹, J. P. Liu¹⁷, H. B. Liu^{4g}, J. Liu¹, Q. Liu¹⁵, R. G. Liu¹, S. Liu⁸, Z. A. Liu¹, F. Lu¹, G. R. Lu⁵, J. G. Lu¹, C. L. Luo⁹, F. C. Ma⁸, H. L. Ma², Q. M. Ma¹, M. Q. A. Malik¹, Z. P. Mao¹, X. H. Mo¹, J. Nie¹, S. L. Olsen¹⁵, R. G. Ping¹, N. D. Qi¹, J. F. Qiu¹, G. Rong¹, X. D. Ruan⁴, L. Y. Shan¹, L. Shang¹, C. P. Shen¹⁵, X. Y. Shen¹, H. Y. Sheng¹, H. S. Sun¹, S. S. Sun¹, Y. Z. Sun¹, Z. J. Sun¹, X. Tang¹, J. P. Tian¹⁴, G. L. Tong¹, G. S. Varner¹⁵, X. Wan¹, L. Wang¹, L. L. Wang¹, L. S. Wang¹, P. Wang¹, P. L. Wang¹, Y. F. Wang¹, Z. Wang¹, Z. Y. Wang¹, C. L. Wei¹, D. H. Wei³, Y. Weng^{1h}, N. Wu¹, X. M. Xia¹, G. F. Xu¹, X. P. Xu⁶, Y. Xu¹⁰, M. L. Yan¹⁶, H. X. Yang¹, M. Yang¹, Y. X. Yang³, M. H. Ye², Y. X. Ye¹⁶, C. X. Yu¹⁰, C. Z. Yuan¹, Y. Yuan¹, Y. Zeng⁷, B. X. Zhang¹, B. Y. Zhang¹, C. C. Zhang¹, D. H. Zhang¹, H. Q. Zhang¹, H. Y. Zhang¹, J. W. Zhang¹, J. Y. Zhang¹, X. Y. Zhang¹², Y. Y. Zhang¹³, Z. X. Zhang¹¹, Z. P. Zhang¹⁶, D. X. Zhao¹, J. W. Zhao¹, M. G. Zhao¹, P. P. Zhao¹, Z. G. Zhao¹⁶, B. Zheng¹, H. Q. Zheng¹¹, J. P. Zheng¹, Z. P. Zheng¹, B. Zhong⁹, L. Zhou¹, K. J. Zhu¹, Q. M. Zhu¹, X. W. Zhu¹, Y. S. Zhu¹, Z. A. Zhu¹, Z. L. Zhu³, B. A. Zhuang¹, B. S. Zou¹

(BES Collaboration)

¹ Institute of High Energy Physics, Beijing 100049, People's Republic of China² China Center for Advanced Science and Technology (CCAST), Beijing 100080, People's Republic of China³ Guangxi Normal University, Guilin 541004, People's Republic of China⁴ Guangxi University, Nanning 530004, People's Republic of China⁵ Henan Normal University, Xinxiang 453002, People's Republic of China⁶ Huazhong Normal University, Wuhan 430079, People's Republic of China⁷ Hunan University, Changsha 410082, People's Republic of China⁸ Liaoning University, Shenyang 110036, People's Republic of China⁹ Nanjing Normal University, Nanjing 210097, People's Republic of China¹⁰ Nankai University, Tianjin 300071, People's Republic of China¹¹ Peking University, Beijing 100871, People's Republic of China¹² Shandong University, Jinan 250100, People's Republic of China¹³ Sichuan University, Chengdu 610064, People's Republic of China¹⁴ Tsinghua University, Beijing 100084, People's Republic of China¹⁵ University of Hawaii, Honolulu, HI 96822, USA¹⁶ University of Science and Technology of China, Hefei 230026, People's Republic of China¹⁷ Wuhan University, Wuhan 430072, People's Republic of China¹⁸ Zhejiang University, Hangzhou 310028, People's Republic of China

^a Current address: Zhengzhou University, Zhengzhou 450001, People's Republic of China

^b Current address: Johns Hopkins University, Baltimore, MD 21218, USA

^c Current address: University of Oklahoma, Norman, Oklahoma 73019, USA

^d Current address: Jinan University, Jinan 250022, People's Republic of China

^e Current address: National Natural Science Foundation of China, Beijing 100085, People's Republic of China

^f Current address: University of Hong Kong, Pok Fu Lam Road, Hong Kong

^g Current address: Graduate University of Chinese Academy of Sciences, Beijing 100049, People's Republic of China

^h Current address: Cornell University, Ithaca, New York 14853, USA

Abstract

Using a data sample with a total integrated luminosity of 10.0 pb^{-1} collected at center-of-mass energies of 2.6, 3.07 and 3.65 GeV with BESII, cross sections for e^+e^- annihilation into hadronic final states (R values) are measured with statistical errors that are smaller than 1%, and systematic errors that are about 3.5%. The running strong interaction coupling constants $\alpha_s^{(3)}(s)$ and $\alpha_s^{(5)}(M_Z^2)$ are determined from the R values.

1 Introduction

The R ratio is defined as the lowest level hadronic cross section normalized by the theoretical $\mu^+\mu^-$ production cross section in e^+e^- annihilation

$$R = \frac{\sigma_{had}^0(e^+e^- \rightarrow \gamma^* \rightarrow \text{hadrons})}{\sigma_{\mu\mu}^0(e^+e^- \rightarrow \gamma^* \rightarrow \mu^+\mu^-)}, \quad (1)$$

and it is an important input parameter for precision tests of the Standard Model (SM). The errors on R value measurements below 5 GeV have a strong influence on the uncertainties of the calculated QED running electromagnetic coupling constant $\alpha(s)$, the muon anomalous magnetic moment ($g-2$) and global SM fits for the Higgs mass [1, 2, 3]. In addition, precision measurements of R values between 2.0 and 3.7 GeV provide a test of perturbative QCD and QCD sum rule calculations [4, 5, 6].

In 1998 and 1999, R value measurements were made at 91 energy points [7, 8] between 2 and 5 GeV by the BESII [9] experiment. The R values were determined from the expression

$$R_{exp} = \frac{N_{had}^{obs} - N_{bg}}{\sigma_{\mu\mu}^0 L \epsilon_{trg} \epsilon_{had}^0 (1 + \delta_{obs})}, \quad (2)$$

where N_{had}^{obs} is the number of observed hadronic events, N_{bg} is the number of QED background events surviving hadron selection (e^+e^- , $\mu^+\mu^-$, $\tau^+\tau^-$, $\gamma\gamma$, etc.), L is the integrated luminosity, ϵ_{trg} is the trigger efficiency for hadronic events, ϵ_{had}^0 is the hadronic efficiency without the

simulation of initial state radiation (ISR), and $(1 + \delta_{obs})$ is the effective ISR correction which includes the effect of radiated photons on the hadronic acceptance. The average statistical errors of the R values are 2 – 4%, and the systematical errors are 5 – 8% depending on the energy point; for the latter, the errors associated with the event selection, hadronic efficiency, and luminosity are dominant.

In 2004, large-statistics data samples were accumulated at center-of-mass energies of 2.60, 3.07 and 3.65 GeV; the total integrated luminosity was 10.0 pb^{-1} . An additional 65.2 nb^{-1} was accumulated at 2.2 GeV for the purpose of tuning the parameters of the hadronic event generator. Improvements in the event selection, tuning of generator parameters and luminosity measurement have been made in order to decrease the systematic errors. The previously used EGS-based (Electron Gamma Shower) [10] detector simulation (where hadronic interactions were parametrized but not simulated) was replaced by a GEANT3-based one [11, 12], where both electromagnetic and hadronic interactions are simulated. The consistency between data and Monte Carlo (MC) has been validated using many high purity physics channels [13]. With these improvements, the errors on the new measured R values are reduced to about 3.5%.

In this letter, improvements compared to the previous measurements are described, and the error analysis and results are reported. Finally, the strong running coupling constant $\alpha_s^{(3)}(s)$ and $\alpha_s^{(5)}(M_Z^2)$ are determined from the R values.

2 Data analysis

The analysis used for this work is similar to that used in the previous BESII R measurements [7, 8]. Two large sources of error in the measurement arise from the event selection and the determination of the hadronic efficiency; these are strongly correlated.

2.1 Selection of hadronic events

In the BEPC energy region, data collected include processes that originate from beam-beam collisions, $e^+e^- \rightarrow e^+e^-, \mu^+\mu^-, \tau^+\tau^-, \gamma\gamma, e^+e^-X$ (X means any possible final state), and hadrons (including continuum and resonant states), as well as beam associated backgrounds. The observed final state charged particles are e, μ, π, K , and p . To test the hadron selection criteria, described below, different types of backgrounds are selected using specialized criteria, and most of them are rejected with good efficiency [7, 8, 14].

The candidate hadronic events are classified by their number of charged tracks. The selection of hadronic events is done in two successive steps: one at the track level and the other at the event level.

(I) Track level: only charged tracks that are well fitted to a helix are considered; the point of closest approach of the track, signified by (V_x, V_y, V_z) , must be within 2 cm of the beam-line in the x - y plane with no restriction on V_z ; the angle between the track and the z axis is limited by the coverage of the main drift chamber (MDC) to be within $|\cos \theta| < 0.84$; a momentum cut $p < E_b(1 + 0.1\sqrt{1 + E_b^2})$ removes tracks with unphysically high momentum (E_b is the beam energy in units of GeV); a time of flight (TOF) requirement $t_{TOF} \leq t_p + 2 \text{ ns}$ is applied

to reject events with unphysical times (t_p is the expected value for a proton with momentum p); the energy deposited in the barrel shower counter (BSC), E_{BSC} , must be less than the minimum of 1 GeV and $0.6E_B$; and the number of hit layers in the muon counter must be smaller than 3.

A neutral cluster in the BSC is considered to be a photon candidate if the angle between the nearest charged track and the cluster is greater than 25° ; the difference between the angle of the cluster development direction and the photon emission direction in the BSC is less than 30° ; and the number of hit layers in the BSC is larger than two.

(II) Event level: the requirement that the total deposited energy, E_{BSC}^{sum} , is greater than the maximum of 0.5 GeV and $0.28E_b$ eliminates most of the beam-associated backgrounds. The selected tracks must not all point into the forward ($\cos\theta > 0$) or the backward ($\cos\theta < 0$) hemisphere. For multi-track events ($n_{ch} \geq 3$), no further requirement is used. For two-track events, the two charged tracks cannot be back-to-back, so the angle between them is required to be less than 165° , and there must be at least two isolated photons with energy $E_\gamma > 0.1$ GeV that are well separated from charged tracks, *i.e.* the distance between the neutral and charged tracks at the first layer of the BSC must be larger than 34 cm in the x - y plane, or larger than 60 cm in the z direction.

The above described selection criteria for hadronic events with $n_{ch} \geq 2$ are almost the same as used in the previous measurements [7, 8]. In the BEPC energy region, the number of events with one observed/reconstructed charged track in BESII accounts for about 8-13% of all hadronic events. The omission of one-track (and zero-track) hadronic events introduces some uncertainty in the tuning the parameters of the hadronic event generator parameters; this in turn induces a sizable systematic error in the hadronic efficiency. However, for single-track events, contamination from beam-associated backgrounds is significant. Therefore, a more restrictive hadronic event selection is applied [14]: the event must have one charged track that is well fitted to a helix (the event can have additional any number of charged tracks with poor helix fits). If this charged track is identified as e^\pm , the event is rejected. If its momentum is in the range $p > 1$ GeV and the number of hit layers in the muon counter is larger than 1, the event is also rejected. For each single-track event, the number of photons with energy $E_\gamma > 0.1$ GeV should be two or more. To further suppress background from fake photons, only events with one well fitted charged track and at least one reconstructed π^0 are considered as single-track hadronic events. A 1-C fit is applied under the $\pi^0 \rightarrow \gamma\gamma$ hypothesis. For candidates with more photons ($n_\gamma \geq 3$), the $\gamma\gamma$ pair combination with the smallest χ^2 is chosen. The χ^2 probability for the 1-C fit is required to be larger than 1%. Figure 2(h) shows the invariant $\gamma\gamma$ mass distribution for one-track events satisfying requirements for data and MC (the MC is normalized to the integrated luminosity of the data). The good agreement indicates that the rate of one-track events in data and MC are commensurate, and the residual beam-associated background is small.

For selected events, the weighted average vertex position, \bar{V}_z , is determined using

$$\bar{V}_z = \frac{\sum_{i=1}^n V_z(i)/\tilde{\chi}_i^2}{\sum_{i=1}^n 1/\tilde{\chi}_i^2}, \quad (3)$$

where $V_z(i)$ is the z coordinate of the i th selected track, χ_i^2 is the track fitting chi-square,

$\tilde{\chi}_i^2 = \chi_i^2/n_{D.O.F.}$, $n_{D.O.F.}$ is the number of degrees of freedom, and n is the number of tracks in the event. Figure 1 shows the \bar{V}_z distributions for candidate hadronic events (including the residual beam-associated and QED backgrounds) at 2.6, 3.07 and 3.65 GeV. Signal events produced by e^+e^- collisions originate near the collision point (in the neighborhood of $z = 0$), and the non-beam-beam backgrounds, such as those from beam-gas and beam-wall scattering, are distributed all along the beam direction (In order to show the shape of the \bar{V}_z distribution of residual beam-associated backgrounds clearly, a logarithmic vertical scale is used). The number of observed hadronic events N_{had}^{obs} is determined by fitting the \bar{V}_z distribution with a Gaussian to describe the hadronic events and an m -th degree polynomial for the residual beam associated backgrounds.

The numbers of residual QED background events, N_{bg} in Eq.(2), are determined from MC simulations using QED event generators with an accuracy of 1% [15], where

$$N_{bg} = L[\epsilon_{ee}\sigma_{ee} + \epsilon_{\mu\mu}\sigma_{\mu\mu} + \epsilon_{\tau\tau}\sigma_{\tau\tau} + \epsilon_{\gamma\gamma}\sigma_{\gamma\gamma}]. \quad (4)$$

Here σ_{ee} is the production cross section for Bhabha events given by the corresponding generator, ϵ_{ee} is the efficiency for Bhabha events that pass the hadronic event selection criteria, and other symbols have corresponding meanings. The values of ϵ_{ee} and $\epsilon_{\mu\mu}$ are about 5×10^{-4} , and $\epsilon_{\tau\tau}$ is 36.45% at 3.65 GeV. The errors on N_{bg} are given in Table 2. The amount of background from $e^+e^- \rightarrow e^+e^-X$ that survives hadron selection is much smaller than 1% of N_{bg} and is neglected.

2.2 Tuning the LUARLW parameters

The hadronic efficiency is determined using the LUARLW hadronic event generator [16]. The physical basis of LUARLW is the Lund area law [17]. The production of hadrons is described as the fragmentation of a semi-classical relativistic string [18], and the quark components of the string and decays of unstable particles are handled by subroutines in JESTSET [19, 20, 21].

Both generators LUARLW and JETSET have some phenomenological parameters that have to be determined from data. The important parameters in JETSET are $PARJ(1 - 3)$, which are responsible for the suppression of diquark-diantiquark pair production, quark pair production, and the extra suppression of strange diquark production respectively, and $PARJ(11 - 17)$, which control the relative probabilities of different spin mesons. The values of these parameters have been tuned with LEP data, as well as with information from lower energy e^+e^- colliders [22]. The generator LUARLW has also been tuned with BES data taken at 2.2, 2.6, 3.07 and 3.65 GeV. The tuned parameters for the Lund area law are mainly the dynamical parameter b and those related to the initial multiplicity distributions (including neutral clusters and charged tracks) from the string decay [16].

The basic method is to find a set of parameters that make various distributions (especially those related to the hadronic selection) simulated by MC agree well with experimental data at all of the measured energy points. The distributions used for the data–MC comparison are: the multiplicities of charged tracks and neutral clusters, the V_{x-y} and V_z coordinates of charged tracks, the charged track momentum, the polar-angle θ between tracks and the beam

direction, the deposited energy in the BSC, the time of flight, and fractions of π^\pm , K^\pm , and some other short-lived particles (π^0 , K_S , ϕ , Λ), etc.. With these distributions, the systematic errors corresponding to each criteria used in the hadronic event selection can be determined. Figure 2 shows, for example, some comparisons between data and the LUARLW MC at 3.65 GeV, where reasonable agreement is evident. More distributions at other energy points are also compared, which can be found in Refs. [14, 23].

The parameters for detector simulation are studied using data. The constant files for dead and hot channels, and the detailed detector responses are inputs for detector simulations.

2.3 Trigger, luminosity and ISR

The trigger conditions are almost the same as those used for the R measurements reported in Refs. [7, 8], and the details about the values and errors of the trigger efficiency are described in Refs. [24]. Since one-track hadronic events are also included in this measurement, the TOF back-to-back hit trigger requirement is not used, thereby making the trigger conditions somewhat looser than before. The trigger table used in data taking is given in Ref. [14]. The trigger efficiencies ϵ_{trg} for hadronic events is determined as 99.8%, and its associated errors is conservatively estimated to be 0.5%.

The integrated luminosity L is measured with wide-angle ($|\cos\theta| < 0.6$) Bhabha events. The measurement method is similar to that described in Refs.[7, 8]. The Bhabha events are selected using only BSC information, and the simulation of the BSC is significantly improved by the package (SIMBES) described in [13], which provides better consistency between MC and data. In addition, the BSC selection efficiencies, determined by simulation, are corrected using correction factors determined with another Bhabha sample, that is selected using only MDC information. The efficiency correction factors range from 0.994 to 1.026 with an uncertainty of about 1.4% for the different energy points. In addition, the contribution from $e^+e^- \rightarrow \gamma\gamma$ is subtracted explicitly. As a result, the precision of the luminosity determined is significantly improved, and the systematic uncertainties are about 2%. For example, at 2.6 GeV the systematic error is 1.9%, of which the trigger efficiency contributes 0.5%, the MC generator 0.5%, event selection 1.2%, and the Bhabha correction 1.3%.

An $\mathcal{O}(\alpha^3)$ Feynman-diagram-based calculation for the initial state radiative (ISR) correction is used in both the calculation of the ISR factor ($1 + \delta_{obs}$) and the simulation of radiative events by LUARLW. A detailed description of the ISR treatment can be found in Refs. [25, 26, 27, 28, 29]. In the ISR simulations and calculations, the contributions from both continuum and resonances are considered. The inclusive hadronic cross section below 5 GeV uses the experimental value, and above 5 GeV uses the theoretical value predicted by QCD [30]. The quantities related to the narrow J/ψ and ψ' are treated analytically.

Figure 3 shows the detection efficiencies for hadronic events simulated with LUARLW for the cases where an initial-state e^+ or e^- radiates a photon with energy fraction $k \equiv E_\gamma/E_b$ and those events with $n_{ch} \geq 1$ are selected. Curves fitted to $\epsilon(k)$ are used in the calculation of $(1 + \delta_{obs})$ at different energies. The values of $(1 + \delta_{obs})$ and their errors are listed in Tables 1 and 2, respectively.

3 Error analysis

The Feynman-diagram-based ISR simulated angle and momentum distributions for the radiated photon are built into LUARLW, which allows the hadronic efficiency $\bar{\epsilon}_{had}$ including radiative effects to be obtained, averaging over the ISR spectrum. The number of hadronic events N_{had}^{obs} , the hadronic efficiency $\bar{\epsilon}_{had}$, and their errors are correlated. The equivalent number of hadronic events, which corresponds to the number of hadronic events produced at the collision point, is defined as

$$N_{had} = \frac{N_{had}^{obs}}{\bar{\epsilon}_{had}}. \quad (5)$$

The combined systematic error associated with the event selection and hadronic efficiency is denoted as ΔN_{had} . This error is caused by discrepancies between data and MC samples for the hadronic selection criteria discussed in Section 2.1. In addition, an uncertainty associated with the parameters of the MC hadronization model is estimated to be about 1% by comparing different sets of tuned parameters, and is included in the error of the hadronic event efficiency.

The error on N_{had}^{obs} due to the choice of the degree of the polynomial used in the fitting is less than 0.7%. The fit errors for N_{had}^{obs} , which are calculated from the uncertainties in the fitted parameters of the Gaussian signal peaks, are 1.34% at 2.6 GeV, 1.11% at 3.07 GeV, and 0.73% at 3.65 GeV. The total ΔN_{had} is the quadratic sum of all fractional errors.

The uncertainty in the effective ISR factor $(1 + \delta_{obs})$ due to errors of the hadronic cross sections at the different effective energies for radiative events is considered (the errors on the hadronic cross section given in the PDG06 tables [30] are used); these decrease with increasing energy from 0.9% to 0.1%. For comparison, another approach based on structure functions [31] is also used at all energy points. The differences in the values of $(1 + \delta)$ for the two schemes are smaller than 1.1%.

A conclusion of the KLN theorem is that the radiative corrections due to final state radiation (FSR) are negligible for a measurement of the inclusive hadronic cross section that sums over all hadronic final states [32]. At the present level of precision, the FSR correction factor in Eq.(2) can be neglected. However, the absence of final state radiation in the event generator introduces some error into the determination of the hadronic event detection efficiency. The masses of the produced hadrons in the final states are much greater than that of the initial radiative e^\pm . As a result, the effect of FSR is much weaker than initial bremsstrahlung. Its influence is estimated to be 0.5% and is included in the error.

The 0-track hadronic events are not selected in this analysis, and the influence of 0-track events on the parameter tuning of LUARLW is not considered. This introduces some error into the hadronic event efficiency determination. Events with no charged tracks cannot be well separated from background. The fraction of 0-track events is estimated from the MC to be 3.4% at 2.6 GeV, 2.9% at 3.07 GeV, and 2.4% at 3.65 GeV. If the difference for 0-track events between MC and data is conservatively assumed to be 20%, the errors for the lost/unobserved 0-track events are 0.7%, 0.6% and 0.5%, respectively. The error related to 0-track events is included into the error of N_{had} defined in Eq. (5).

In this analysis, hadronic events are classified according to their number of charged tracks. Therefore, errors in the tracking efficiency σ_{trk} , the differences in the track reconstruction

efficiency between data and MC, introduce some error into the classification and counting of the number of events. For an event with n_{ch} charged tracks, the probability that n_{er} of n_{ch} tracks are wrongly constructed roughly obeys a binomial distribution $B(n_{er}; n_{ch}, \sigma_{trk})$, where the parameter $\sigma_{trk} \sim 2\%$ is the tracking efficiency error at BESII. The R value measurement is, in fact, a counting of the number of hadronic events, so only those cases where all n_{ch} tracks in an event are incorrectly reconstructed ($n_{er} = n_{ch}$) will introduce an error into ΔN_{had} . Considering the distribution of charged multiplicity $P(n_{ch})$ for the inclusive hadronic sample (such as shown in Figure 2(a)), the effective error of tracking efficiency is

$$\Delta\epsilon_{trk} = \sum_{n_{ch} \geq 1} P(n_{ch}) B(n_{er} = n_{ch}; n_{ch}, \sigma_{trk}). \quad (6)$$

The estimated values of $\Delta\epsilon_{trk}$ are listed in Table 2. Since the fraction of single-track events decreases with increasing center-of-mass energy, the error $\Delta\epsilon_{trk}$ also decreases with energy.

The errors on the R values are determined with Eq. (2) (including all errors analyzed in last section and estimated by Eq. (6)). The final R values are $2.18 \pm 0.02 \pm 0.08$ at 2.6 GeV, $2.13 \pm 0.02 \pm 0.07$ at 3.07 GeV, and $2.14 \pm 0.01 \pm 0.07$ at 3.65 GeV, which are summarized in Table 1.

As a cross check, the R values are determined using the relation

$$R_{exp} = \frac{N_{had}^{obs} - N_{bg}}{\sigma_{\mu\mu}^0 L \epsilon_{trg} \bar{\epsilon}_{had} (1 + \delta)}, \quad (7)$$

where $\bar{\epsilon}_{had}$ is the hadronic efficiency averaged over all of the ISR spectrum, and $(1 + \delta)$ is the corresponding theoretical ISR factor. The ISR scheme used to simulate $\bar{\epsilon}_{had}$, ϵ_{had}^0 and to calculate $(1 + \delta)$ and $(1 + \delta_{obs})$ are the same in order to keep the consistency between theoretical calculation and simulation. The R values determined with Eq. (7) are $2.17 \pm 0.01 \pm 0.07$ at 2.6 GeV, $2.13 \pm 0.01 \pm 0.07$ at 3.07 GeV, and $2.16 \pm 0.01 \pm 0.08$ at 3.65 GeV. The mean R values obtained using Eqs. (2) and (7) are consistent to within 1%.

A cross check is also made by selecting hadronic events with $n_{ch} \geq 2$ as was done in Refs. [7, 8]. In this case, the R values at the three energy points are $2.20 \pm 0.02 \pm 0.08$, $2.13 \pm 0.02 \pm 0.07$, and $2.15 \pm 0.01 \pm 0.08$, respectively. The differences in the mean R values determined by selecting hadronic events with $n_{ch} \geq 1$ and $n_{ch} \geq 2$ are consistent within 1%.

4 Results and discussion

Tables 1 and 2 list the quantities used in the determination of R using Eq. (2) and the contributions to the total error. The results are shown in Fig. 4, together with previous measurements. The errors on the R values reported here are about 3.5%. The R values are consistent within errors with the prediction of perturbative QCD [4].

Compared with our previous results [7, 8], the measurement precision has been improved due to three main refinements to the analysis: (1) the simulation of BES including both of the hadronic and electromagnetic interactions with a GEANT3 based package SIMBES that has a more detailed geometrical description and matter definition for the sub-detectors; (2) large

data samples are taken at each energy point, with statistical errors smaller than 1%; (3) the selected hadronic event sample is expanded to include one-track events, which supplies more information to the tuning of LUARLW, and results in the improved values of parameters and hadronic efficiency.

In another BESII work, parts of the data sample taken at 3.65 GeV with a luminosity of 5.536 pb^{-1} and at 3.665 GeV with a luminosity of 998.2 nb^{-1} are used, the hadronic events with more than 2-tracks ($n_{ch} \geq 3$) are selected, and the averaged R value is $R = 2.218 \pm 0.019 \pm 0.089$ which has an error of 4.1% [33].

Based on the R values in this work and the perturbative QCD expansion that computes $R_{QCD}(\alpha_s)$ to $\mathcal{O}(\alpha_s^3)$ [34], the strong running coupling constant $\alpha_s^{(3)}(s)$ can be determined at each energy point [35, 36]. The obtained $\alpha_s^{(3)}(s)$ values are evolved to 5 GeV, and the weighted average of the measurements $\bar{\alpha}_s^{(4)}(25 \text{ GeV}^2)$ is listed in Table 3. When evaluated at the M_Z scale, the resulting value is $\alpha_s^{(5)}(M_Z^2) = 0.117^{+0.012}_{-0.017}$, which agrees with the world average value within the quoted errors [4].

Table 1: Items used in the determination of R at each energy point.

$E_{cm}(\text{GeV})$	$L(\text{pb}^{-1})$	N_{had}^{obs}	N_{bg}	$\epsilon_{had}^0(\%)$	$(1 + \delta_{obs})$	R	σ_{sta}	σ_{sys}
2.60	1.222	24026	193	63.81	1.08	2.18	0.02	0.08
3.07	2.291	33933	208	67.63	1.11	2.13	0.02	0.07
3.65	6.485	83767	4937	71.83	1.21	2.14	0.01	0.07

Table 2: Summary of the systematic errors (%).

$E_{cm}(\text{GeV})$	L	N_{had}	N_{bg}	$\Delta\epsilon_{trk}$	ϵ_{trg}	$(1 + \delta_{obs})$	Total
2.60	2.00	2.79	0.05	0.32	0.50	1.18	3.68
3.07	1.96	2.53	0.05	0.29	0.50	1.15	3.45
3.65	1.38	2.74	0.35	0.26	0.50	1.10	3.33

Table 3: $\alpha_s(s)$ determined from R values at 2.600, 3.070, and 3.650 GeV, and evolved to 5 GeV. The first and second errors are statistical and systematic, respectively. Shown in the last two columns are the weighted averages of the three measurements at 5 GeV and M_Z .

$\sqrt{s}(\text{GeV})$	$\alpha_s^{(3)}(s)$	$\alpha_s^{(4)}(25\text{GeV}^2)$	$\bar{\alpha}_s^{(4)}(25\text{GeV}^2)$	$\alpha_s^{(5)}(M_Z^2)$
2.60	$0.266^{+0.030+0.125}_{-0.030-0.116}$	$0.212^{+0.018+0.068}_{-0.019-0.086}$	$0.209^{+0.044}_{-0.050}$	$0.117^{+0.012}_{-0.017}$
3.07	$0.192^{+0.029+0.103}_{-0.029-0.101}$	$0.169^{+0.022+0.074}_{-0.023-0.086}$		
3.65	$0.207^{+0.015+0.104}_{-0.015-0.104}$	$0.189^{+0.012+0.082}_{-0.013-0.091}$		

The BES collaboration thanks the staff of BEPC and computing center for their hard efforts. BES collaboration also thanks B. Andersson for helping in the development of generator LUARLW during 1998-1999. This work is supported in part by the National Natural Science Foundation of China under contracts Nos. 19991480, 19805009, 19825116, 10491300, 10225524, 10225525, 10425523, 10625524, 10521003, the Chinese Academy of Sciences under contract No. KJ 95T-03, the 100 Talents Program of CAS under Contract Nos. U-11, U-24, U-25, and the Knowledge Innovation Project of CAS under Contract Nos. U-602, U-34 (IHEP), the National Natural Science Foundation of China under Contract No. 10225522 (Tsinghua University), and the Department of Energy under Contract No. DE-FG02-04ER41291 (U. Hawaii).

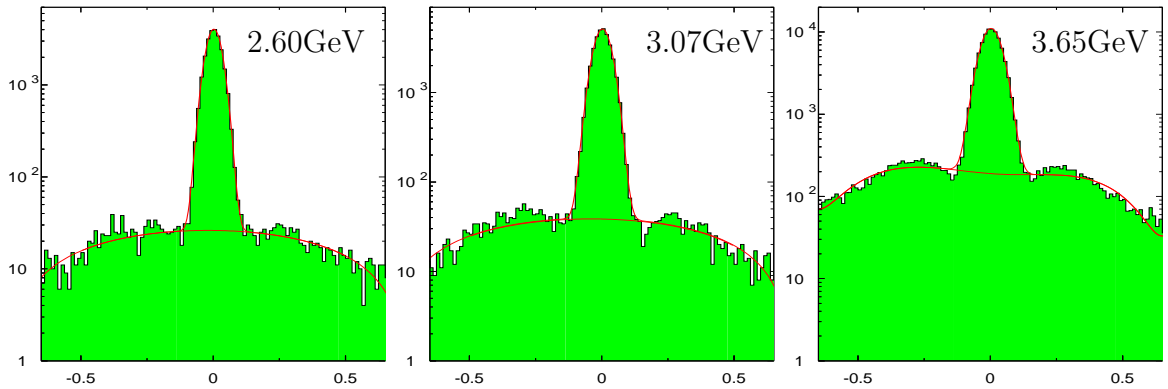


Figure 1: Distributions of \bar{V}_z for candidate hadronic events. The distributions are fitted by a Gaussian to represent the signal and a polynomial to describe the residual beam-associated backgrounds.

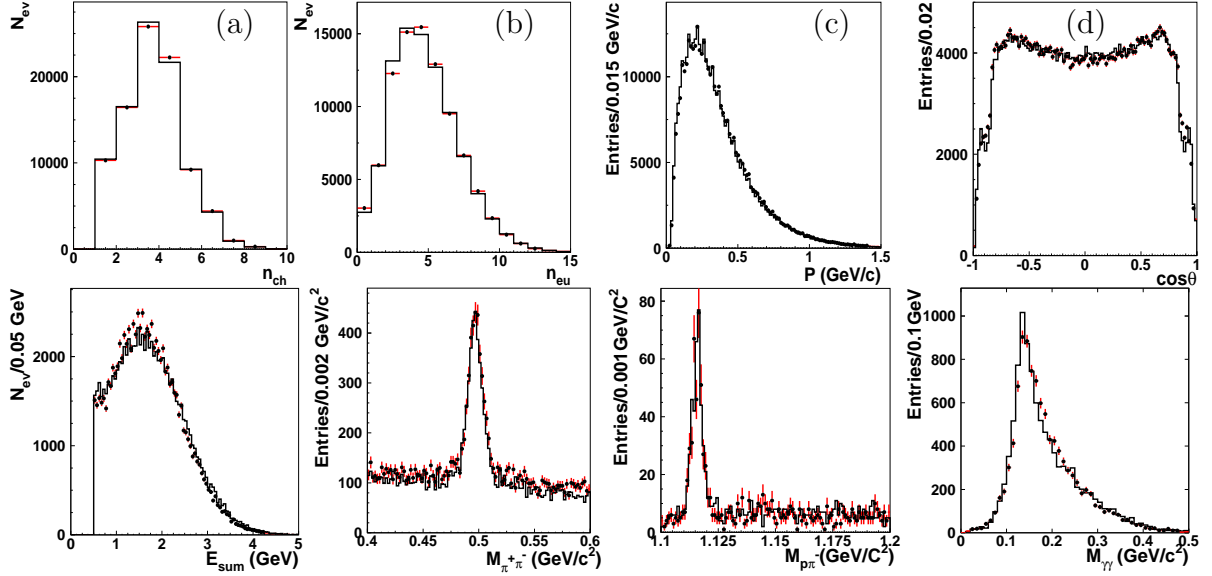


Figure 2: The normalized distributions for data (dots with error bars) and the LUARLW MC (histograms) at 3.65 GeV with full detector simulation. From left to right and upper to down are: (a) multiplicity of charged tracks; (b) multiplicity of neutral clusters; (c) momenta p of charged tracks; (d) polar-angles between charged tracks and beam direction, $\cos\theta$; (e) deposited energies in the BSC; invariant masses of (f) $K_S \rightarrow \pi^+\pi^-$; (g) $\Lambda \rightarrow p\pi^-$ and (h) $\pi^0 \rightarrow \gamma\gamma$ decays respectively.

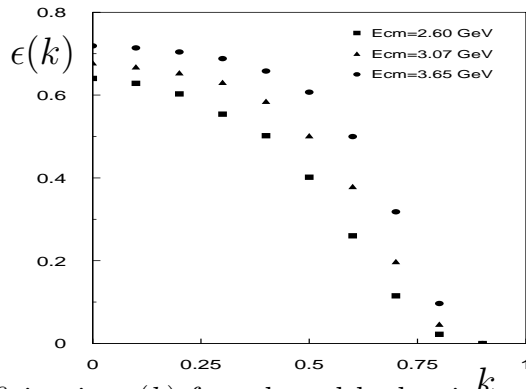


Figure 3: Radiative efficiencies $\epsilon(k)$ for selected hadronic k events with $n_{ch} \geq 1$ at some values of k .

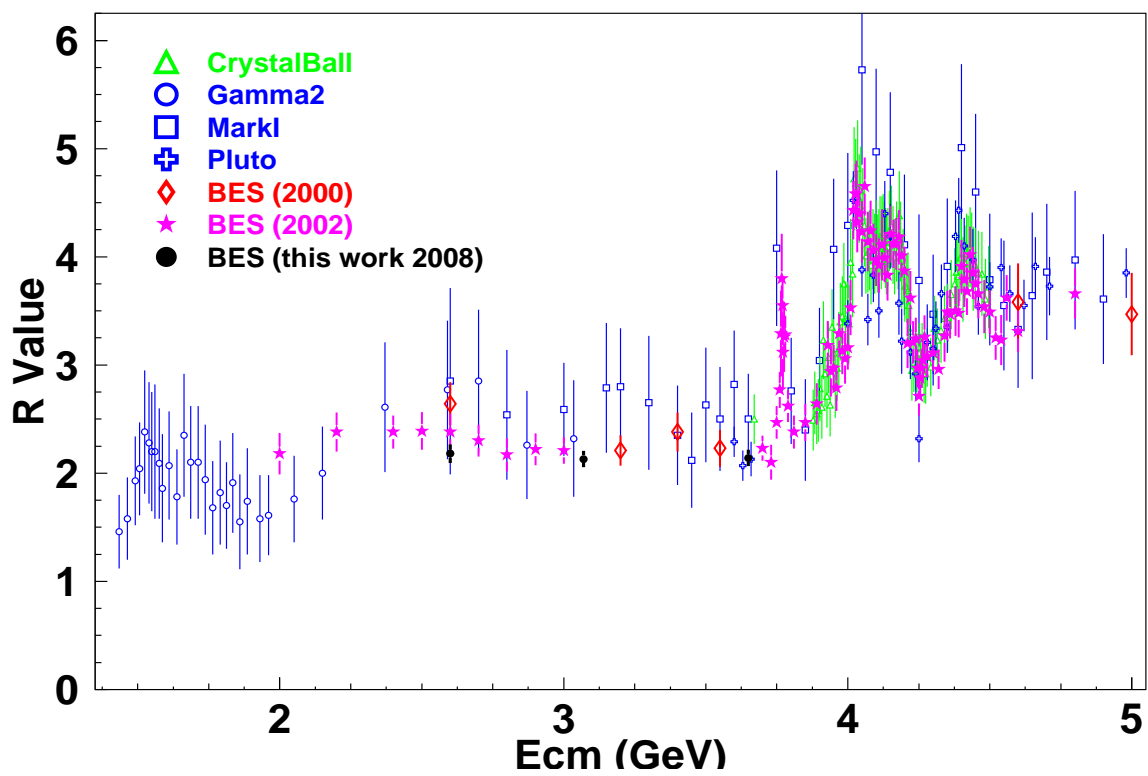


Figure 4: R values reported here together with previous measurements below 5 GeV.

References

- [1] B. Pietrzyk, Nucl. Phys. B (Proc. Suppl.) **162**, 18 (2006).
- [2] F. Jegerlehner, Nucl. Phys. B (Proc. Suppl.) **162**, 22 (2006).
- [3] F. Ambrosino *et al.*, hep-ex/0603056, and references therein.
- [4] C. Amsler *et al.*, Phys. Lett. B **667**, 122 (2008).
- [5] M. Davier *et al.*, Phys. Lett. **B 419**, 419 (1998).
- [6] M. Davier *et al.*, Eur. Phys. J. **C 27**, 497 (2003).
- [7] J.Z. Bai *et al.*, BES Collaboration, Phys. Rev. Lett. **84**, 594 (2000).
- [8] J.Z. Bai *et al.*, BES Collaboration, Phys. Rev. Lett. **88**, 101802 (2002).
- [9] J. Z. Bai *et al.*, BES Collaboration, Nucl. Instr. Meth. A **458**, 627 (2001).
- [10] W. R. Nelson *et al.*, The EGS4 Code System, SLAC-265, 1992.
- [11] CERN Program Library Long Writeup W5013, CERN, Geneva, Switzerland, 1993.
- [12] <http://wwwasdoc.web.cern.ch/wwwasdoc/>.
- [13] M. Ablikim *et al.*, BES Collaboration, Nucl. Instrum. Meth. A **552**, 344 (2005).
- [14] H. Hu *et al.* High Energy Physics and Nuclear Physics **31**, 802 (2007).
- [15] These generators are based on the calculation by the references: F. A. Berends *et al.*, Nucl. Phys. **B57**, 381 (1973); Nucl. Phys. **B68**, 451 (1974); Nucl. Phys. **B177**, 237 (1981); Nucl. Phys. **B228**, 537 (1983).
- [16] H.M. Hu *et al.*, High Energy Phys. and Nucl. Phys. **25**, 1035 (2001) (in Chinese).
- [17] B. Andersson and H. Hu, hep-ph/9810285.
- [18] B. Andersson, The Lund Model, Cambridge University Press (1998).
- [19] T. Sjöstrand, CERN-TH.7112/93.
- [20] T. Sjöstrand, Computer Physics Commun. **39**, 347 (1986).
- [21] T. Sjöstrand, Computer Physics Commun. **43**, 367 (1987).
- [22] Armin Böhrer, Phys. Rep. **191**, 107 (1997).
- [23] Y. Weng *et al.*, High Energy Physics and Nuclear Physics **31**, 703 (2007).
- [24] G.S.Huang *et al.*, High Energy Physics and Nuclear Physics **25**, 889 (2001)

- [25] A. Osterheld et al., SLAC-PUB-4160 (1986).
- [26] C. Edwards et al., SLAC-PUB-5160 (1990).
- [27] H. Hu et al., High Energy Physics and Nuclear Physics **25**, 701 (2001).
- [28] G. Bonneau and F. Martin, Nucl. Phys. **B27**, 381 (1971).
- [29] F. A. Berends and R. Kleiss, Nucl. Phys. **B178**, 141 (1981).
- [30] Particle Data Group, Jour. Phys. **33**, (2006)116
- [31] E. A. Kureav and V. S. Fadin, Sov. Nucl. Phys. **41**, 466 (1985).
- [32] Y. S. Tsai, SLAC-PUB-3129, May 1983.
- [33] M. Ablikim *et al.*, BES Collaboration, Phys. Lett. **B641**, 145 (2006).
- [34] S. G. Gorishnii, *et al.*, Phys. Let. **B259**, 144 (1991).
- [35] J. H. Kühn and M. Steinhauser, arXiv:hep-ph/0109084 v3 (2002).
- [36] J. Hu et al., High Energy Physics and Nuclear Physics **31**, 1 (2007).